International Journal of Research in Engineering and Science (IJRES)
ISSN (Online): 2320-9364, ISSN (Print): 2320-9356
www.ijres.org Volume 13 Issue 3 ǁ March 2025 ǁ PP. 98-104

Design and Analysis of Dual Band Circularly Polarized THz Planar Slot MIMO Antenna for B5G/6G and Nano Communications

Sanjeev Kumar Saxena[1*]
[1]*Department of Mathematics, N.M.S.N. Dass (P.G.) College, Budaun, U.P., India, 243601*

Abstract:
In this article, a novel two-port dual-band dual-circularly polarized THz Planar slot antenna with diversity is designed for 6G application. The antenna consists of a square slot, two asymmetric T-shaped feed lines in orthogonal direction protrude from signal lines, and an arrow shaped grounded stub at the inner corner of the ground slot between the two orthogonal feed lines at an angle of 45°. Orthogonal feed lines are used for generation of circular polarized waves. If we apply the excitation at another port the sense of circular polarization is interchange in both the bands of axial ratio. The lower band of axial ratio covers frequency range of 1.28-2.32THz with 58.11% and fc_1=1. 80THz.Same for upper band covers frequency range of 3.34–3.51 THz with 5.03% and fc_2=3.42THz. The two ports of antenna have isolation more than 15 dB and 20dB in the lower and upper band of axial ratio. The proposed antenna has both circular polarized bands within the impedance bandwidth.
Keywords: *Multi-port antenna, dual-band, dual-sense of polarization, axial ratio, circular polarization, polarization diversity, slot antenna, CPW feed line.*

Date of Submission: 09-03-2025 Date of acceptance: 23-03-2025

I. INTRODUCTION

OVER the past few decades, wireless data rates have increased significantly, which has prompted scrutiny to go into the electromagnetic spectrum's least-explored regions to meet user data needs. In order to address the need of capacity limits, the Sub-THz (0.1-0.3 THz) and THz frequency ranges (0.3-10 THz) are therefore taken into consideration. This frequency band is anticipated to accommodate 6 G wireless communication technologies in the future. [1]. Due to its numerous uses, including imaging, spectroscopy, remote sensing, ultra-high precision location, and future wireless communications like T-WLAN, T-WPAN, etc., it has also drawn interest from the research community worldwide. The Sub THz band of frequencies, which offer a high data rate, enable extremely rapid downloading speeds for computer communications, video conferencing, and holographic gaming, among other things. [2–5]. The attenuation and propagation losses caused by the atmosphere must be overcome when designing an antenna for the Sub-THz range of frequencies. Low profile antennas with strong gain and wide bandwidth are preferred to reduce these losses. [6]. The implementation of an antenna in the terahertz region of frequency can be accomplished using a variety of techniques, including an on-chip silicon layer, a patch antenna, a Yagi Uda, a Luneburg lens, a silicon micro lens, and a substrate integrated waveguide antenna [7-12]. On-chip antennas are simple to combine with other circuits, however because of the lossy substrate, they have a lower efficiency. Utilizing a patch antenna at THz is significantly hampered by severe metallic and dielectric losses as well as the presence of surface current. High gain is accomplished in Yagi Uda by using linear dipole components including reflectors, directors, and feeding elements [13]. Circularly polarized waves can reduce polarization losses between the transmitting and receiving antennas, hence dual band antennas for CP are recommended since they can be utilized in multiband applications simultaneously. There are two forms of polarization sensing in dual band printed antennas for CP, single sense [14-18] and dual sense [15-26]. The dual-sense antennas come in handy for applications that call for dual-sense reception of both left- and right-hand circular polarization signals. In the event where the spacing between the two frequency bands is narrow, the isolation between the two frequency bands in a dual-sense antenna is superior to a single sense antenna. This research article introduces a novel two-port antenna. Use two asymmetric T-shaped feed lines in orthogonal direction protrude from signal lines, and an arrow shaped grounded strip at the left inner side of the slot between the orthogonal asymmetric signal line. The axial ratio generated at the lower band due to the orthogonally nature of the signal line. Due to the mirror image symmetry the sense of polarization is interchangeable by changing the port of excitation.

II. PROPOSED CONFIGURATION OF ANTENNA:

The schematic representation of the antenna structure (70um × 70 um x 1.6 um) and photograph of antenna is shown in Fig.1 and its structural dimensions are shown in caption of fig.1. In the ground plane, a square slot is etched and it is fed with a 50Ω feed line of 3.2um of width which is kept at a 0.7um distance from the ground plane.

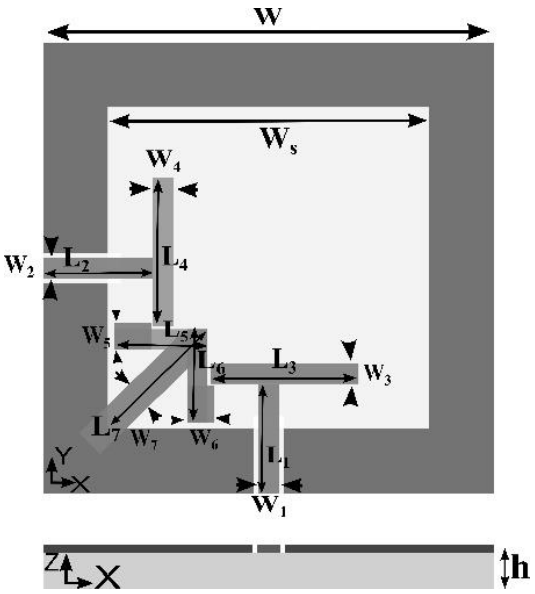

Fig.1. Schematic representation of the antenna structure.

(W=70, Ws=50, L_1=17, W_1=3.2, L_2=17, W_2=3.2, L_3=23, W_3=3.2, L_4=23, W_4=3.2, L_5=14.5, W_5=4.2, L_6=14.5, W_6=4.2, L_7=22, W_7=4.6 and h=1.6) (Unit: micrometers).

The antenna is modelled using Arlon AD410 (tm) substrate with 1.6um height, the relative dielectric constant, εr = 4.1, and loss tangent = 0.003. The width W_s of the slot is approximately half-wavelength at f_{01}. As shown in Fig. 5, the upper band at f_{02} is due to the next higher order mode of the rectangular slot. It has square slot ground plane, two signal lines normal to each other and an arrow shaped stub connected to slot at 45° between two normal lines. One-line works as stub in normal direction w.r.t other line, when the signal is applied to the any port.

III. THE EVOLUTION OF ANTENNA GEOMETRY AND ANALYSIS

Antenna evolution steps are explained by four prototypes in Figure 2(a). Antenna 1 has two orthogonally oriented signal lines and a square slot ground plane; Antenna 2 includes a grounded stub connected at the inner corner of the slot; Antenna 3 includes an arrow shaped stub connected at the inner corner of ground plane; and Antenna 4 further includes modified strips width of arrow shaped stub. By placing two orthogonally oriented signal lines as shown in Antenna 1 and applying signal at one port same time other port is matched with 50Ω. The matched port's signal line work as a stub in the normal direction of excited port's line. This results in the generation of circular polarization waves as shown in Fig. 2(d). Then, one stub is connected to the ground slot to improve axial ratio at lower band and to generate CP in upper band as shown in Antenna 2. Giving the arrow head shape to grounded stub by adding two another stubs, enhance and improve the axial ratio bandwidths at lower and upper bands as shown in Antenna 3. In Antenna 4, further modification in lower axial ratio bandwidth is done by tuning the size of arrow head shaped stub. Their simulated results are shown in Figure 2(b), (c) & (d).

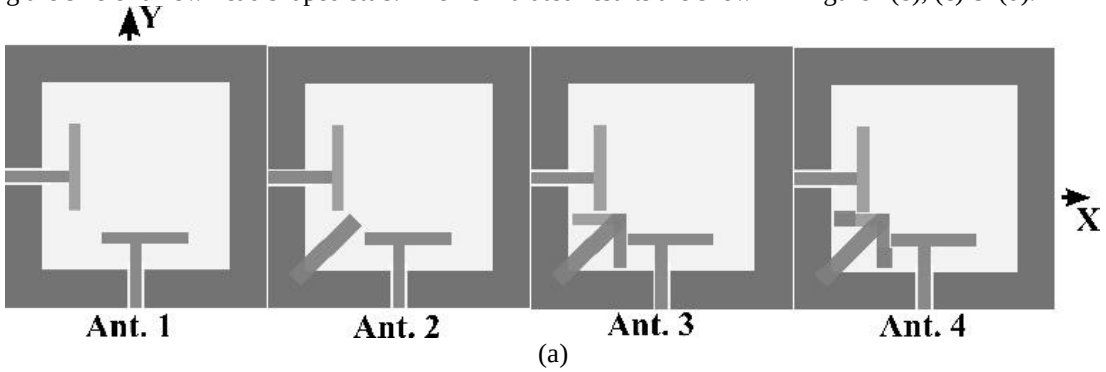

(a)

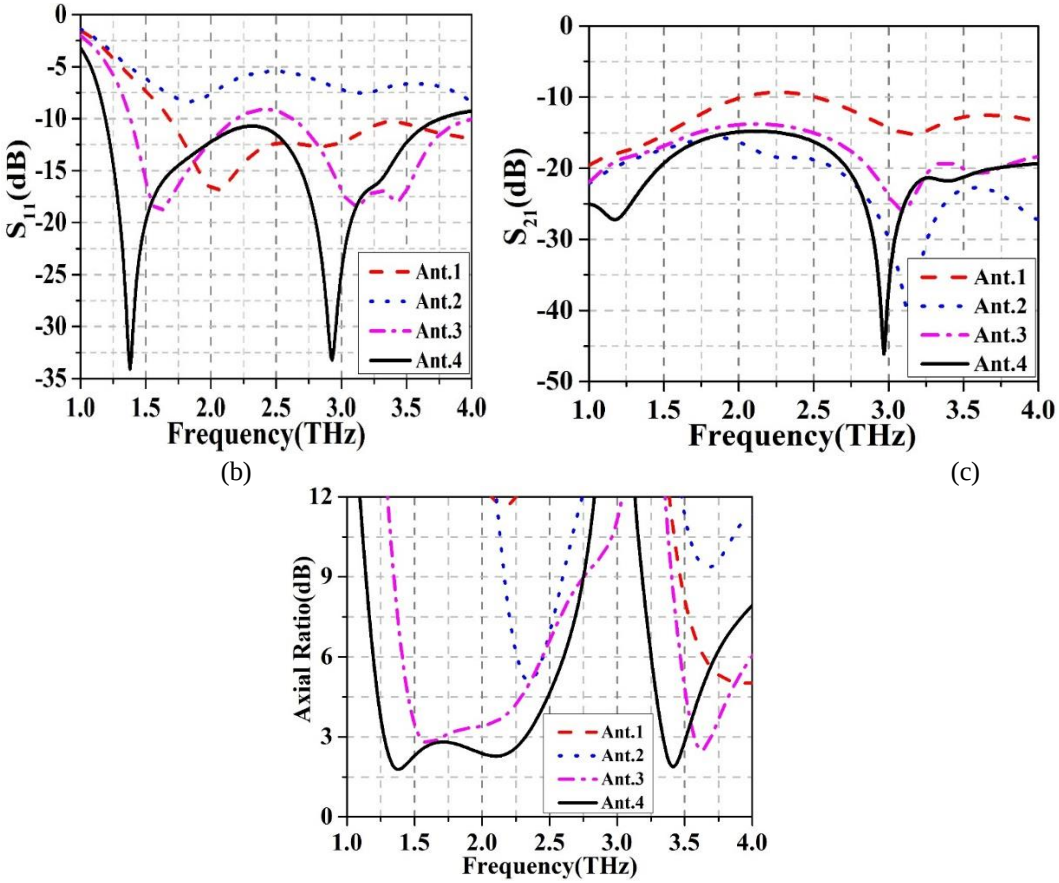

Fig. 2(a) Steps of prototypes: (b) Simulated results of reflection coefficients, (c) Isolation and (d) Axial ratios: of prototypes.

IV. MECHANISM OF THE PROPOSED DUAL CP ANTENNA

To verify the generation of dual CP radiation, the simulated surface magnetic current distributions of the proposed dual CP antenna at 1.8, and 3.42 THz are illustrated in Figure 3. The proposed antenna is designed to realize RHCP and LHCP in +z direction for lower and upper band of axial ratio respectively.

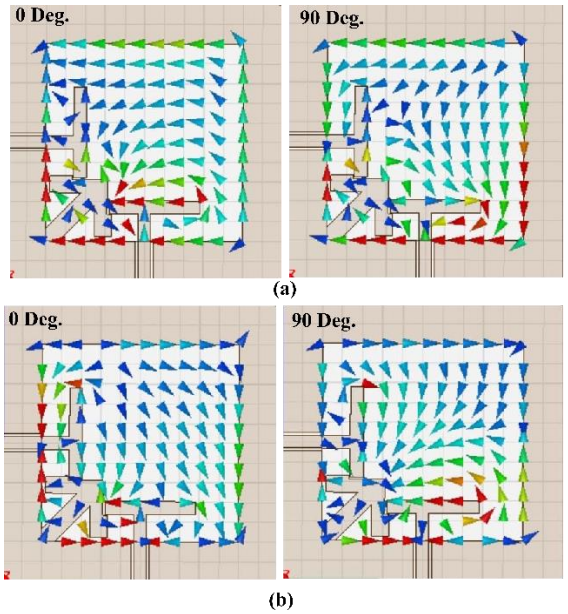

Figure 3. Magnetic current distributions of proposed antenna: (a) 1.8 THz, and (b) 3.42 THz. (Excitation at port 1)

The surface currents at 1.8 THz are shown in Figure 3 (a). At 1.8 THz the direction of magnetic currents is in anticlockwise for the top view (+z). So, the CP wave is produced by the proposed antenna is RHCP in nature. The 0° phase shows that the superimposed current is -x directed with φ is 45°. For 90° phase, the current is in -y directed with φ is 45° and for 180° phase, current is in opposite direction to the current at 0° phase. The current direction of 270° phase is opposite to the current at 90° phase. The surface currents at 3.42 THz are shown in Figure 3 (b). It can be seen that the CP waves are generated by the magnetic currents rotating in clockwise direction results in LHCP radiation. At 3.42 THz, for 0° phase the superimposed current is along -y direction with φ is -45°. The 90° phase the current is along -y direction with φ is 45°. For 90° phase the current is along -x direction with φ is 45°. The 180° phase surface current is opposite to the current phase at 0° phase and the 270° phase surface current is opposite to the current at 90° phase. With the help of parametric observation of various parameters, the influence on the $S_{11,}$ S_{21} and AR bandwidth has been observed. The parametric observation is presented in figure 4 shows the simulated curves with different optimized values of $L_{3,}$ L_4, W_5 *and* W_6. From the figures 4a, 4b and 4c, it can be clear that this variable mainly affects the impedance bandwidths in the operating band.

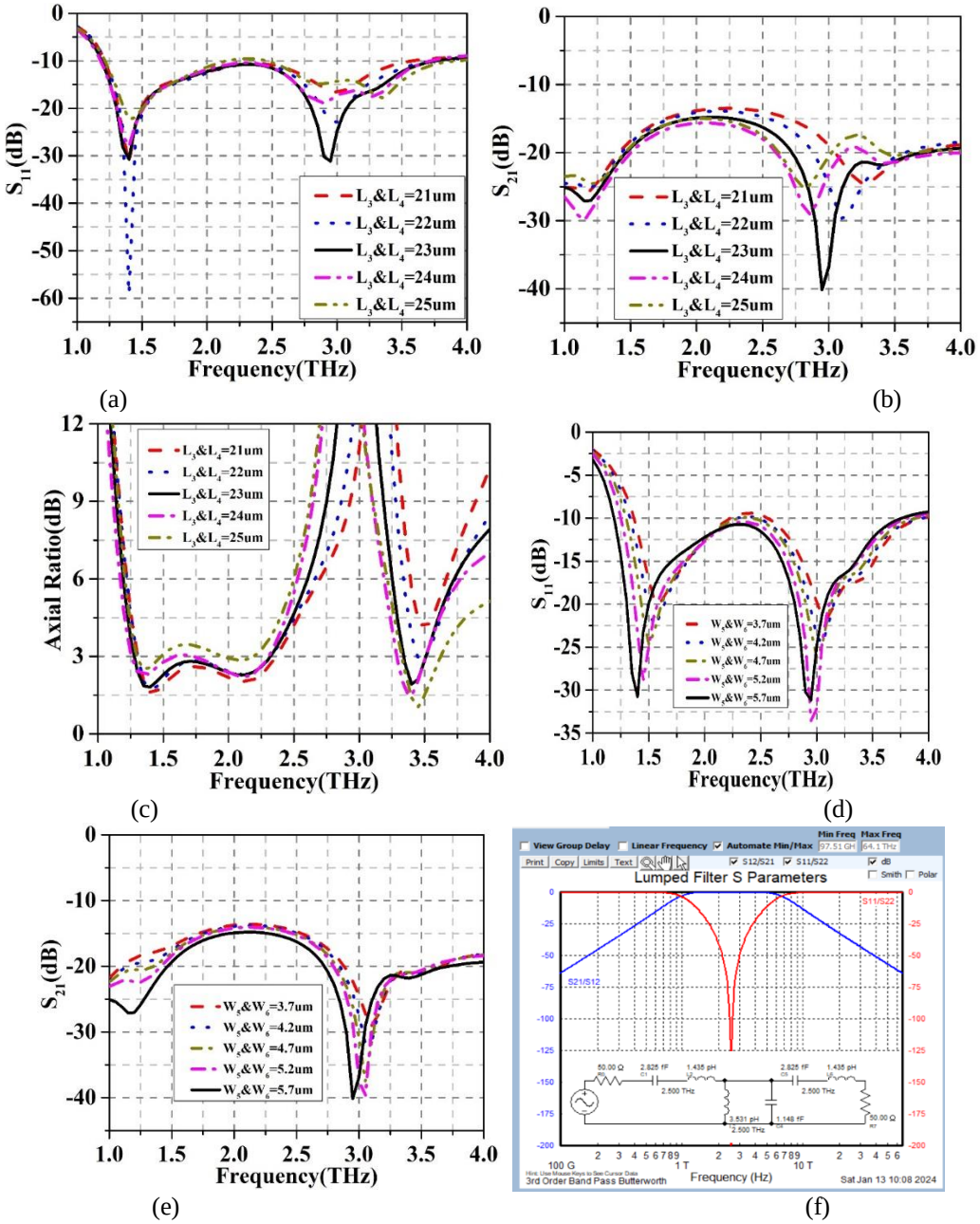

Fig. 4. Variation of parameters L3, L4, W5 and W_6: (a) Reflection coefficients (L3 & L4), (b) the isolation (L3 & L4), (c) Axial ratios (L3 & L4), (d) Reflection coefficients (W5 & W_6), (e) the isolation (W5 & W_6) and (f) Electrical equivalent diagram with S_{11}/S_{21} Graph

Next, the effect of the widths of the strips of arrow shaped grounded stub is investigated as shown in Fig. 4d, and 4e . The lower cut-off frequency of first band decreases when the widths of (W_5 *and* W_6) becomes higher. This parameter mainly affects the lower band of S_{11} bandwidth, where the upper band is almost same and lower cut-off frequency of lower band changes significantly. From Fig. 4(e), it can be seen that the increments in widths W_5 and W_6 has ability to shifts the axial ratio bands to lower frequency side. When the feed lines length is fixed at L_3 *and* L_4 *=23*um, the desired bandwidth of the proposed antenna can be achieved. It is observed that keeping L_5, L_6*=14.5um*, L_7*=22um* and W_5, W_6*=5.7um* the axial ratio bandwidths lies within the impedance bandwidths with good isolation in terms of impedance bandwidths and port isolation.Fig.4(f) provides the information about how much series inductance and series capacitance and parallel inductance and capacitance to be added in conductor (Patch)- dielectric and dielectric-conductor(ground) medium with respect to 50Ω resistance. Total series and parallel capacitance and inductance value extracted by empherical formula, Cseries=2.825fF, Lseries=1.435pH and Cparallel=1.148fF, Lparallel=3.531pH at 2.75THz centre frequency.

V. RESULTSAND DISCUSSIONS

The impedance and isolation curves are shown in figure 5(a). The S_{11}(dB) bandwidths of antenna covers the frequencies from 1.19THz to 3.76THz (103.84% & fc=2.475THz) covers both axial ratio bands. Figure 5(b) depicts the axial ratio against frequency. The axial ratio bandwidths are about 58.11% (1.28–2.32 THz) at lower band and 5.03% (3.34–3.51 THz) at upper band, where S_{11}(dB) is below -10dB. The isolation S_{21}(dB) varies from 15 to 24dB and 20 to 21dB in lower and upper band of axial ratio. Figure 5(c) depicts the gain against frequency that varies from 1.74dB to 4.43dB and 3.5dB to 3.85dB in lower and upper axial ratio bandwidth. For the good performance of antenna for diversity in radiation pattern the value of ECC should be less than 0.5. It is good for a two-port antenna that ECC should remain below 0.5 as shown in fig.5(d) [24-27]. The proposed antenna satisfies this condition for entire axial ratio bandwidth. A closed cavity of suitable size and a reflector at the back side of antenna are used for further improvement of gain and cross polarization of the antenna. Fig. 6(a) & (b) show the radiation patterns of the antenna at 1.8THz and 3.42THz (Port 1 excitation). The cross polarization is approximately greater than 18dB in the direction of maximum radiation (+z dir).

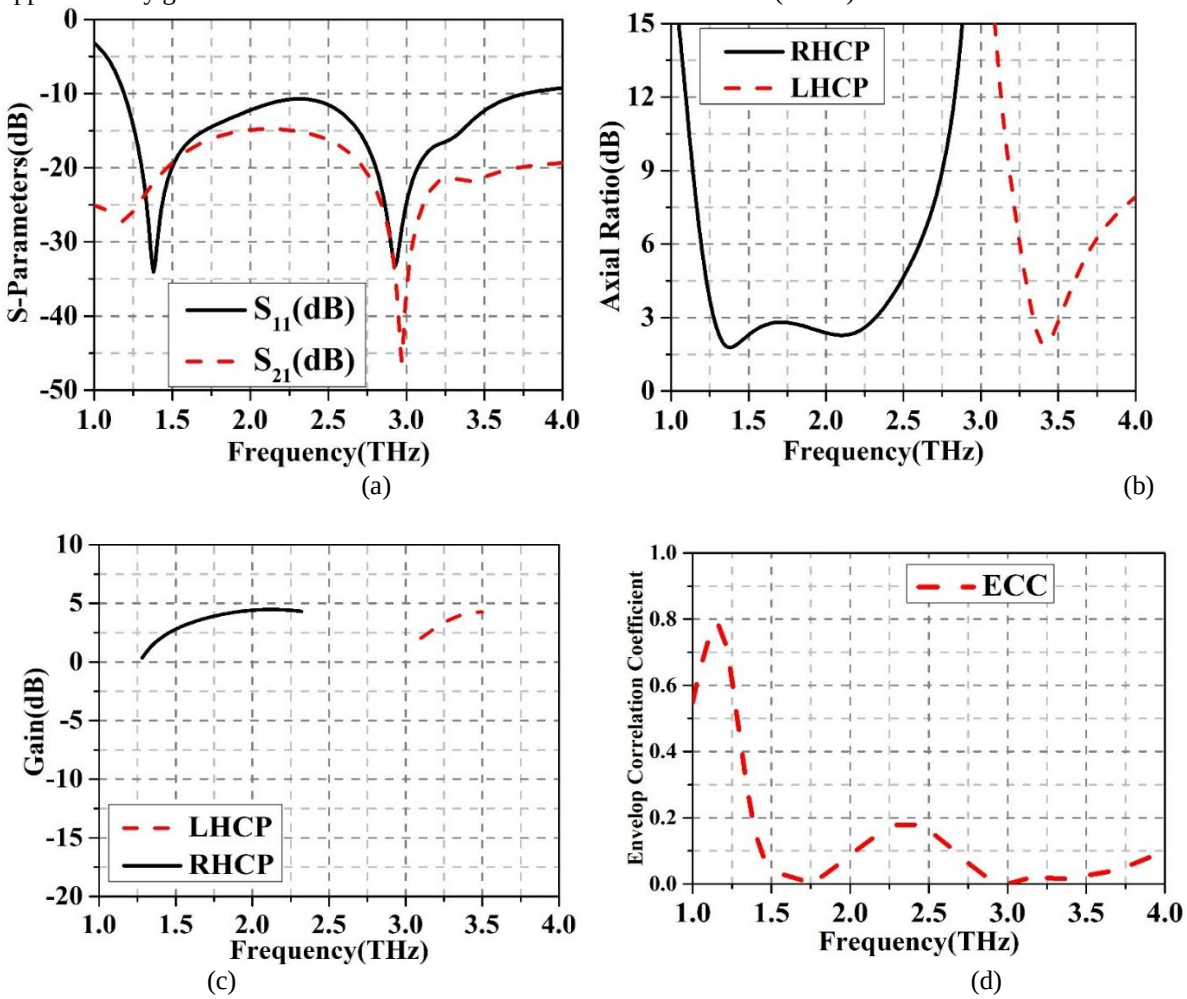

Fig. 5. (a) Reflection coefficient and port isolation, (b) axial ratio, (c) Gain, and (d) ECC.

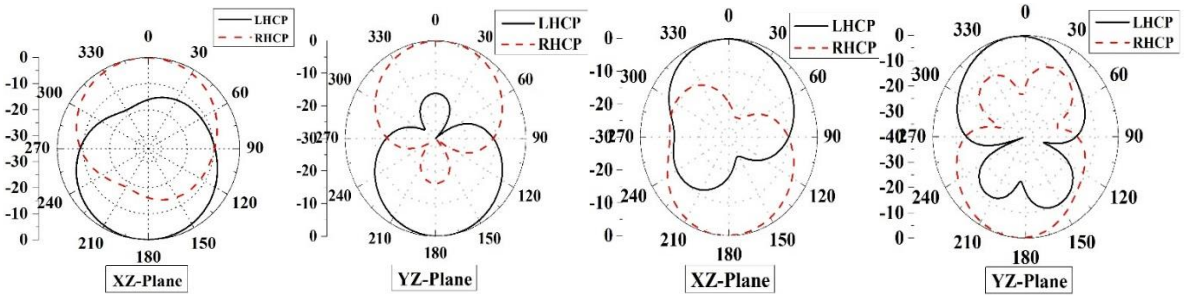

(a) (b)

Figure 6. (a) Rradiation patterns at1.8THz and (b) 3.42THz (Excitation in port 1)

VI. CONCLUSION:

A dual band dual circularly polarized square slot antenna with polarization diversity in both band having good isolation fed by a CPW has been presented. The return loss is better than 10 dB at both the bands and there is isolation between the lower and upper bands of impedance bandwidth. The isolation varies from 15 to 21 dB at lower band and 21–25 dB at upper band. Proposed MIMO antenna also circularly polarized in dual band having left hand and right hand in nature for vehicular communication. Therefore, this proposed antenna is suitable for polarization diversity application in the given axial ratio bands of THz frequency range for 6G application.

REFERENCES

[1] Zahraa R.M. Hajiyat, Alyani Ismail, Aduwati Sali, Mohd Nizar Hamidon, Antenna in 6G wireless communication system: specifications, challenges, and research directions, Optik 231 (2021), 166415.
[2] P.H. Siegel, Terahertz technology, IEEE Trans. Microw. Theory Technol. 50 (3) (2002) 910–928.
[3] Theodore S. Rappaport, Yunchou Xing, Ojas Kanhere, Shihao Ju, Arjuna Madanayake, Soumyajit Mandal, Ahmed Alkhateeb, Georgios C. Trichopoulos, "Wireless communications and applications above 100 GHz: Opportunities and challenges for 6G and beyond" , IEEE Access 7 (2019) 78729–78757.
[4] Ian F. Akyildiz, Josep Miquel Jornet, Chong Han, Terahertz band: next frontier for wireless communications, Phys. Commun. 12 (2014) 16–32.
[5] Ho-Jin Song, Tadao Nagatsuma, Present and future of terahertz communications, IEEE THz Sci. Technol. 1 (1) (2011) 256–263.
[6] Muhammad Ali Jamshed, Ali Nauman, Muhammad Ali Babar Abbasi, Sung Won Kim, Antenna selection and designing for THz applications: suitability and performance evaluation: a survey, IEEE Access 8 (2020) 113246–113261.
[7] Mohammad Alibakhshikenari, Bal S. Virdee, Mohsen Khalily, Chan H. See, Raed Abd-Alhameed, Francisco Falcone, Tayeb A. Denidni, Ernesto Limiti, High gain on-chip antenna design on silicon layer with aperture excitation for terahertz applications, IEEE Antennas Wirel. Propag. Lett. 19 (9) (2020) 1576–1580.
[8] U. Keshwala, S. Rawat, K. Ray, Inverted K-shaped antenna with partial ground for THz applications, Optik 219 (2020), 165092.
[9] Lars Josefsson, A waveguide transverse slot for array applications, IEEE Trans. Antennas Propag. 41 (7) (1993) 845–850.
[10] T.A. Nisamol, K.K. Ansha, P. Abdulla, Design of sub-THz beam scanning antenna using Luneburg lens for 5G communications or beyond, Prog. Electromagn. Res. C 99 (2020) 179–191.
[11] María Alonso-DelPino, N.úria Llombart, G. Chattopadhyay, Craig Lee, Cecile Jung-Kubiak, L. Jofre, Imran Mehdi, Design guidelines for a terahertz silicon microlens antenna, IEEE Antennas Wirel. Propag. Lett. 12 (2013) 84–87.
[12] K.K. Ansha, P. Abdulla, T.A. Nisamol, A.R. Anu, Sub-THz SIW circular ring slot antenna with wide bandwidth and high gain, IEEE-Hydcon., pp. 1–4, 2020.
[13] Hamsakutty Vettikalladi, Waleed Tariq Sethi, Ahmad Fauzi Bin Abas, Wonsuk Ko, Majeed A. Alkanhal, Mohamed Himdi, Sub-THz antenna for high-speed wireless communication systems, Int. J. Antennas Propag. 2019 (2019) 1–9.
[14] R. K. Saini, and S. Dwari, ―CPW-fed broadband circularly polarized rectangular slot antenna with L-shaped feed line and parasitic elements, Microw. Opt. Technol. Lett., vol. 57, no. 8, pp. 1788–1794, Aug. 2015.
[15] R. K. Saini, and S. Dwari, ―Broadband dual circularly polarized square slot antenna, IEEE Trans. Antennas Propag., vol. 64, no. 1, pp. 290-294, Jan. 2016.
[16] Li, R. L., Bushyager, N. A., Laskar, J., Tentzeris, M. M.: Determination of reactance loading for circularly polarized circular loop antennas with a uniform traveling-wave current distribution. IEEE Trans. Antennas Propag. 53(12), 3920-3929 (2005).
[17] Xu, L., Lu, W.-J., Yuan, C.-Y., Zhu, L.: Dual circularly polarized loop antenna using a pair of resonant even-modes. International Journal of RF and Microwave Computer-Aided Engineering, vol. 29, Issue 6, 1-10, e21703 (2019).
[18] Chen, Z., Hu, W., Gao, Y., Wen, L., Li, C., Hu, Z., Jiang, W., Gao, S.: Compact wideband circularly polarized loop antenna based on dual common and differential modes. IEEE Antenn. Wireless Propag. Lett. 21(8), 1567-1571 (2022).
[19] Shimizu, K., Fujimoto, T.: A printed inverted-F antenna for dual-band dual-sense circular polarization. in Proc. IEEE int. Workshop on Electromagnetics, Japan, p. 92 (2018), https://doi: 10.1109/iWEM.2018.8536656.
[20] Fujimoto, T., Shimizu, K.: A small printed inverted-F antenna for circular polarization. IEICE Trans. Commun. E102-B(2), 197-204 (2019).
[21] Saini, R. K., Bakariya, P. S., & Kumar, P. (2018). Coplanar waveguide fed dual-band, dual-sense circularly polarized square slot antenna. International Journal of RF and Microwave Computer-Aided Engineering, 28, e21503.
[22] Saini, R. K., Dwari, S., & Mandal, M. K. (2017). CPW-Fed dual-band dual sense circularly polarized monopole antenna. IEEE Antennas and Wireless Propagation Letters, 16, 2497–2500.
[23] Saini, R. K. (2019). Polarization reconfigurable dual- band rectangular slot antenna. Journal of RF-Engineering and Telecommunications, Frequenz, 73(9–10), 339–351.
[24] Saxena, Gaurav, Maksud Alam, Manidipa Roy, Abdulwasa Bakr Barnawi, TM Yunus Khan, Ram Lal Yadava, Sanjay Chintakindi, Reena Jain, Himanshu Singh, and Yogendra Kumar Awasthi. "CSRR loaded multiband THz MIMO antenna for nano-communications and bio-sensing applications." Nano Communication Networks 38 (2023): 100481.

[25] Srivastava, Shipra, Saptarshi Gupta, Vibhav Kumar Sachan, Gaurav Saxena, and Satya Sai Srikant. "High gain circularly polarized graphene inspired dielectric resonator antenna for 6G IOT THz optical communication and optical refractive index Biosensing applications." Engineering Science and Technology, an International Journal 49 (2024): 101603.

[26] Saxena, Gaurav, Sanjay Kumar, Sanjay Chintakindi, Abdulsalam Al-Tamim, Mustufa Haider Abidi, Wigdan Aref Mohammed Saif, Sahil Kansal et al. "Metasurface Instrumented High Gain and Low RCS X-Band Circularly Polarized MIMO Antenna for IoT Over Satellite Application." IEEE Transactions on Instrumentation and Measurement (2023).

[27] Saxena, Gaurav, Y. K. Awasthi, and Priyanka Jain. "High isolation and high gain super-wideband (0.33-10 THz) MIMO antenna for THz applications." Optik 223 (2020): 165335.